Electronic Devices

DOI: 10.1002/anie.200501799

In Situ Deposition and Patterning of Single-Walled Carbon Nanotubes by Laminar Flow and Controlled Flocculation in Microfluidic Channels**

*Jang-Ung Park, Matthew. A. Meitl, Seung-Hyun Hur, Monica L. Usrey, Michael S. Strano, Paul J. A. Kenis, and John A. Rogers**

The remarkable electrical, mechanical, and chemical properties of single-walled carbon nanotubes (SWNTs) create interest in their potential use as semiconducting or conducting elements in sensors, nanoscale transistors, and in large-area electronic systems. As a result, considerable research focuses on developing techniques for depositing and patterning SWNTs from solution, as individuals or aggregates, with well-controlled coverage and alignment. Langmuir–Blodgett techniques[1–4] and various schemes of deposition from solution[5–15] have been studied extensively. Although these methods exhibit attractive features, they each have some combination of disadvantages, such as low deposition rate, inability to control tube alignment and/or to deposit over large areas, required chemical modification of the SWNTs or substrates, or the need for organic solvents that are incompatible with plastic device components (organic electrodes, semiconductors, or substrates). A recently described alternative technique uses a controlled flocculation process to drive individual tubes out of an aqueous suspension and onto a substrate.[16] The deposition speed of this approach can be high, the tube coverage (i.e. the number of tubes per unit area) can be controlled over a wide range, and the form of the tubes (isolated individual tubes or bundles) can be defined by the processing conditions. The approach is also compatible with a wide range of substrates and it does not require chemical modification of the tubes or the substrates. However, this method does not allow the local orientation of the deposited nanotubes to be defined in a spatially dependent manner. Depositing and patterning SWNTs in a single step are also difficult, and secondary procedures must be used to transfer the nanotubes onto substrates incompatible with spin coating (e.g., curved surfaces).

Herein we introduce a technique for patterning and depositing SWNTs through the use of controlled flocculation in laminar microfluidic networks. This method generates well-defined patterns of aligned SWNT films with controlled density and alignment on a variety of flat and curved surfaces. We present the essential chemical and physical aspects of this approach, demonstrate the important capabilities, and present examples for use in the fabrication of organic electronic devices.

In the controlled flocculation approach, an aqueous suspension of surfactant-stabilized SWNTs is combined with a solvent, such as methanol, that is miscible with water and exhibits a strong affinity for the surfactant. When the methanol lowers the concentration of surfactant available to interact with the SWNTs to values below the critical micellar concentration, the tubes are no longer well suspended. In this situation, interactions between tubes can lead to the formation of bundles, and interactions with adjacent solid surfaces can cause the tubes to coat these surfaces. The introduction of streams of methanol and aqueous suspensions of SWNTs into a microfluidic channel in which fluid flow is laminar leads to diffusive mixing only near the liquid–liquid interface between the two streams flowing in parallel.[17,18] The interaction between the methanol and the SWNT suspension at this interface leads to the deposition of SWNTs on the solid surfaces near this interface. The velocity profiles of the local flow fields determine the orientation of the tubes. The duration of the flows and their velocities as well as the concentration of the SWNT suspension determine the coverage. Figure 1a shows this process as implemented with microfluidic streams joined by a Y-junction. For the work described herein, we form the fluidic channels by placing a stamp of the elastomer poly(dimethylsiloxane) (PDMS) against the surface of a substrate to be patterned (Figure 1b). Syringe pumps introduce the SWNT solution and methanol

[*] J.-U. Park, M. A. Meitl, S.-H. Hur, Prof. Dr. J. A. Rogers
Department of Materials Science and Engineering
Department of Electrical and Computer Engineering
Department of Chemistry
Beckman Institute, and Frederick Seitz Materials Research Laboratory
University of Illinois at Urbana-Champaign
Urbana, IL (USA)
Fax: (+1) 271-244-1190
E-mail: jrogers@uiuc.edu
M. L. Usrey, Prof. Dr. M. S. Strano, Prof. Dr. P. J. A. Kenis
Department of Chemical & Biomolecular Engineering, and Beckman Institute
University of Illinois at Urbana-Champaign
Urbana, IL (USA)

[**] The authors thank the Center for Nanoscale Chemical Electrical Mechanical Manufacturing Systems at the University of Illinois (funded by the National Science Foundation under grant DMI-0328162) and the Center for Microanalysis of Materials at the University of Illinois (partially supported by the U.S. Department of Energy under grant DEFG02-91-ER45439). M.S.S. acknowledges funding from the U.S. National Science Foundation Career award CTS-0449147.

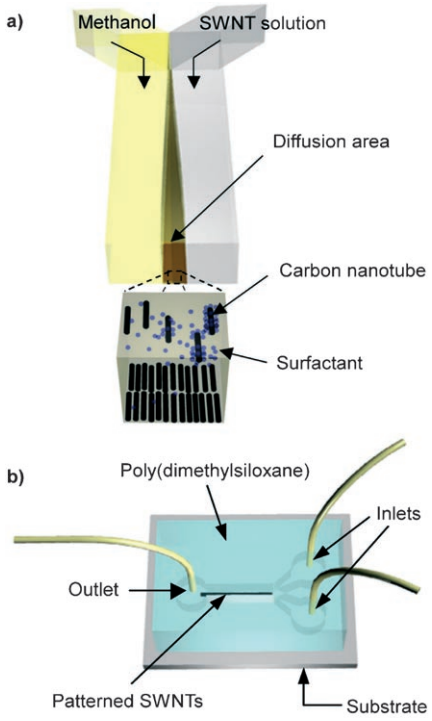

Figure 1. a) A microfluidic Y-junction for patterning single-walled carbon nanotubes (SWNTs) by multiphase laminar flow and controlled flocculation, and b) a microfluidic patterning device built with poly(dimethylsiloxane).

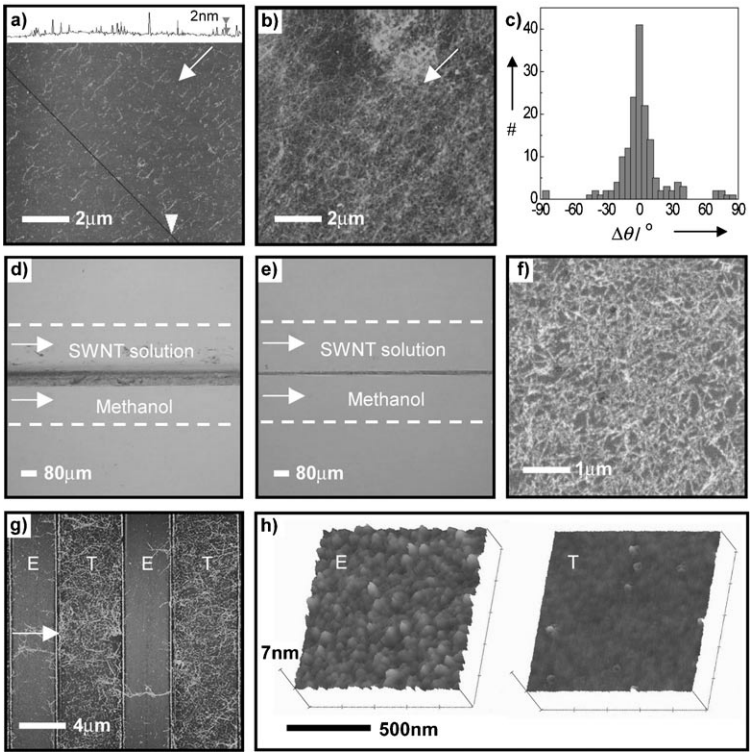

Figure 2. AFM and optical micrograph images of SWNT films fabricated by laminar flow under different flow conditions and substrates. Arrows indicate the flow direction. a) Parallel array of SWNTs deposited onto a Si wafer at an average flow velocity (V_a) of 17 mm s^{-1} for 5 min; tube alignment is in the flow direction. b) SWNTs deposited on a Si wafer at the same velocity ($V_a = 17$ mm s^{-1}) for 15 min showing that coverage of deposited SWNTs increases with flow duration. c) Angular distribution of SWNTs with respect to flow direction in Figure 2a. In this case, # is nanotube count and $\Delta\theta$ is orientation. d) Stripe of SWNTs deposited at an average velocity of 17 mm s^{-1} with methanol (1 mL) and SWNT solution (1 mL). e) Stripe of SWNTs deposited at an average velocity of 170 mm s^{-1} and the same volumes of methanol and SWNT. The width of the stripe decreases with increasing flow velocity. f) SEM image of high-coverage SWNT films patterned in (d). g) AFM image of SWNTs coated onto a surface with patterned lines of electron-beam evaporated (E) and thermally grown (T) SiO_2. The coverage of SWNTs is higher on T-SiO_2 than on E-SiO_2. h) Comparison of the morphology of E-SiO_2 (RMS roughness: 0.535 nm) and T-SiO_2 (RMS roughness: 0.162 nm) surfaces, as measured by AFM.

into the microfluidic networks and accurately control the flow velocities. Peeling the stamp away from the substrate after flowing the liquids for the desired time and washing with methanol and acetone to remove residual surfactant complete the patterning and deposition process.

Figure 2 presents results that illustrate some important aspects of this process. The duration of the flow determines the coverage of the deposited SWNTs. The total volume of methanol and SWNT suspension that flow through a fluidic channel increases linearly with flow duration for constant flow velocity. As a result, the number of deposited SWNTs increases with flow duration. Figures 2a and b show low and high coverage SWNTs formed by short (5 min) and long (15 min) flow durations, respectively. For low coverage, AFM analysis indicates that the SWNTs are present as individual tubes or small bundles. In this case, the SWNTs align parallel to the flow direction (Figure 2c). The full width at half maximum (FWHM) of the angular distribution of SWNT orientation, as measured by analysis of AFM images, is $\approx 10°$ at a flow velocity $V_a = 17$ mm s^{-1}. Carbon nanotubes flowing in a microfluidic channel are affected by shear flow, and hence tubes are aligned in the flow direction.[19,20] As higher flow velocity generates larger shear forces, the degree of alignment increases with V_a.[14,20] For high coverages, the SWNTs have a smaller degree of alignment (Figures 2b, f, and g; part T) than in the case of low-coverage films, for identical flow velocities and substrate surfaces in Figure 2a and c. The relatively thick and nonuniform layers of surfactant that deposit with the SWNTs can frustrate the alignment of SWNTs deposited at the later stages of the process. In all cases, this surfactant was washed away prior to the collection of the AFM images. The flow velocities determine the widths of the patterned stripes of SWNTs (Figures 2d, e, and f). In this case, the SWNTs were deposited with sufficient flow durations that they formed thick films that were visible to the naked eye. Diffusion between the SWNT solution and methanol at the fluidic interface controls the deposition and hence an increase in the flow velocities decreases the diffusion time and, therefore, the widths of the deposited lines of SWNTs. These widths do not depend on the depths of the microfluidic channels significantly. This result suggests that most of the deposited nanotubes originate from locations in the suspension close to the substrate.

We were able to pattern the tubes with this technique onto a wide range of substrates, including plastics,[16,21] without the

need to functionalize the substrates or the tubes with chemistries designed to create strong interactions. (We even observed nanotubes deposited on the low-surface-energy PDMS surfaces of the microfluidic channels, near the interface between the methanol/SWNT suspension.) The details concerning, for example, the degree of alignment or the coverage for a given flow velocity and duration do, however, depend on interactions between the SWNTs and the substrates. As an example, we deposited SWNTs on a substrate with stripes of SiO_2 deposited by electron beam evaporation (E) and thermal oxidation (T) on silicon wafers. The coverage was higher on T-SiO_2 than E-SiO_2 (Figure 2g). We speculate the rough surface of the E-SiO_2 (RMS = 0.53 nm, as measured by AFM) decreased the contact area and, therefore, the interaction strength with SWNTs compared to the relatively smooth surface of the T-SiO_2 (RMS = 0.16 nm; (Figure 2h).[16]

Figure 3 shows other important features of this procedure. The PDMS elements defining the microfluidic channels are mechanically flexible; they can be draped over or bent around curved or uneven surfaces of the type that are difficult to process by spin coating. In this manner, it is possible to deposit and pattern SWNTs with geometries similar to that illustrated in Figure 2 on the curved surfaces of spherical lenses, for example, as shown in Figure 3a. In addition, curvilinear lines, in which the orientation of the SWNTs follows the local tangent, can be patterned by use of microfluidic channels with suitable geometries (Figure 3b). By controlling the relative flow rates of the methanol and the SWNT suspension, the positions of the deposited SWNT stripes can be adjusted relative to the sidewalls of the fluidic channels. Changing the flow rates dynamically during the deposition sweeps the fluidic interface across the channel to generate wide SWNT stripes or multiple, parallel narrow stripes. Figure 3c shows an example of this capability, and a plot of the relative position of the SWNT stripe patterned through the liquid–liquid interface as a function of relative flow rates. Once deposited, the SWNTs adhere sufficiently strongly to most substrates so that they can be further processed by liftoff, etching, etc. by using standard spin cast photoresists as masking layers. Figure 3d shows a narrow gap (10 μm) etched through the center of a deposited SWNT stripe by patterning photoresist, performing reactive ion etching, and then removing the resist. This structure can be used as a pair of electrodes for various applications.

As an example of the ability to build high-quality devices with SWNTs deposited by laminar flow and controlled flocculation, we fabricated organic thin film transistors (OTFTs) in which high-density SWNT networks serve as source/drain electrodes (Figure 4). By controlling the flow duration, SWNT stripes with electrical behavior ranging from insulating (low coverage) to semiconducting (moderate coverage; above percolation threshold for the semiconducting tubes)[16,22–24] to metallic (high coverage; above percolation threshold for the metallic tubes) could be produced. Figure 4a shows the resistivity (ρ) of the deposited SWNT networks (with values as low as $\approx 0.04\ \Omega$ cm) as a function of SWNT solution volume. As coverage of SWNT network increases, more conducting paths are formed and hence the

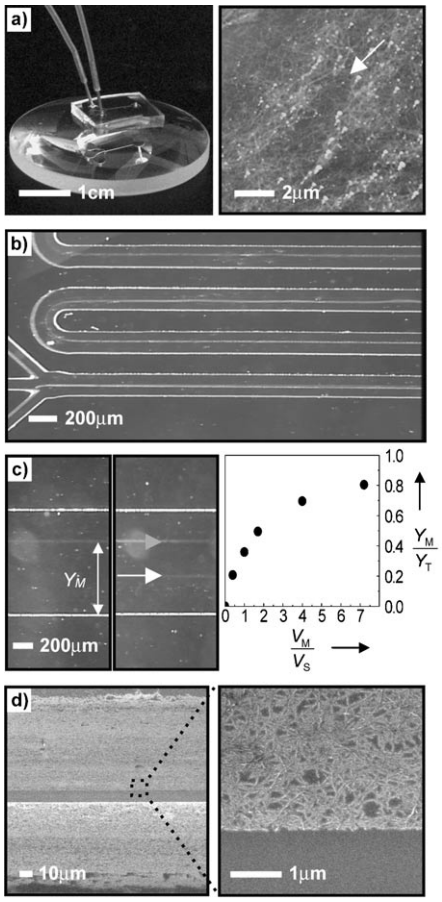

Figure 3. Various patterns of SWNT networks. a) Optical image of a microfluidic patterning system conformably contacted to the curved surface of a lens, and AFM image of SWNTs deposited on this lens (diameter: 4 cm, effective focal length: 10 cm). b) Optical micrograph of an SWNT line deposited in the middle of a serpentine microfluidic channel. c) Optical micrograph of multiple SWNT stripes fabricated in a single channel (channel width: 1 mm, height: 50 μm). Gray and white arrows indicate SWNT stripes patterned first and second, respectively. The position of the SWNT stripe (Y_M/Y_T) is defined by the position of the liquid–liquid interface position, which can be controlled by the flow rate ratio (V_M/V_S) of the two streams (Y_M and Y_T; width of the methanol stream and fluidic channel, and V_S and V_M; flow rate of SWNT solution and methanol, respectively). d) SEM image of SWNT networks deposited over a wide area and then patterned by conventional photolithographic procedures. To form this film, three streams (center stream: SWNT solution, and outside two streams: methanol) flowed in a microfluidic channel (width: 500 μm, height: 50 μm) and the flow rate ratio (V_M/V_S) was changed from 1 to 50 continuously by modulating V_S at constant $V_M = 50\ \mu L\,min^{-1}$. An open gap in the SWNT film was formed by O_2 plasma etching through a photodefined layer of photoresist.

resistivity decreases. This dependence of resistivity on the network coverage can be described by standard percolation theory [Eq. (1)].

$$\log\rho = -\alpha \log (N - N_C) + \text{const} \qquad (1)$$

N is the coverage of the conducting sticks, and N_C is the critical coverage where the first percolative path across a sample is formed. The inset of Figure 4a shows a fit of this

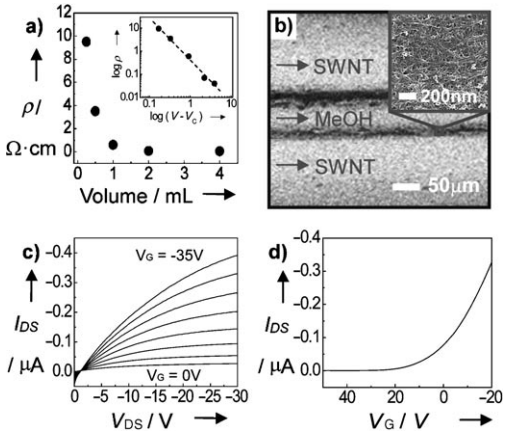

Figure 4. Fabrication of a transistor in which high-coverage SWNT networks patterned by multiphase laminar flow serve as electrodes (source and drain). a) Resistivity of the networks (ρ) as a function of the SWNT solution volume. The inset shows the power fit in the percolation region. b) SEM image of two SWNT network lines patterned in a microfluidic channel using three-phase laminar flows. The inset shows the high coverage SWNT networks that can be produced. These two stripes served as source/drain electrodes of a transistor. The channel length was controlled only by flow velocities of the three fluidic streams. c) Current (I_{DS})–voltage (V_{DS}) characteristics of the SWNT-based OTFT. A thermally evaporated layer (20-nm thick) of pentacene provided the semiconducting layer. d) Gate modulation of I_{DS} in the saturation regime.

equation to our data, using the SWNT solution volume (V) and critical volume (V_C) instead of ($N-N_C$). In this case the experimentally measured value of V_C was 80 μL. This fit yields a value of $\alpha = 1.7$, which is similar to the known values ($1.3 < \alpha < 1.9$) for SWNT networks in two dimensions.[25] For the fabrication of the SWNT-electrode transistor, two lines of high-density SWNT networks with low resistivity ($\approx 0.04\ \Omega$cm) were patterned onto a a highly doped Si wafer with a SiO_2 top layer (gate dielectric, thickness: 300 nm) by three-phase (SWNT solution/methanol/SWNT solution) laminar flow inside a microfluidic channel (height: 50 μm, width: 500 μm; Figure 4b). These two SWNT lines serve as source/drain electrodes; the relative flow velocities of the solutions control the channel length of the transistor (distance between the two SWNT lines: 50 μm). After defining the channel width (250 μm) by O_2 plasma etching, a thin layer of pentacene (thickness: 20 nm) was thermally evaporated onto the electrodes and in the gap at a deposition rate of ≈ 1 Å s^{-1}. Figure 4c and d show the current–voltage (I–V) and transfer characteristics of the resulting SWNT-electrode OTFT. The effective mobility (μ_{eff}), evaluated in the saturation regime (ignoring contacts), and on/off ratio were 0.011 ± 0.001 cm^2 V^{-1} s^{-1} and ≈ 1000:1, respectively. From Figure 4c, the device resistance in the on state (R_{ON}) was 52 ± 7 MΩ at voltage $V_G - V_T \approx -30$ V. The resistance of SWNT source/drain electrodes (R_{SWNT}) was about 2000 times smaller than the R_{ON}. For comparison, we fabricated OTFTs that used pentacene and gold source/drain with the same dimensions as the SWNT device. In this case, μ_{eff} values and on/off ratios of this gold OTFT were similar to those of the SWNT OTFT. The R_{ON} value of the gold-electrode device obtained at the same $V_G - V_T$ voltage was 48 ± 9 MΩ. The parasitic resistance (R_P) of the gold-electrode device was found to be 80 ~ 110 kΩ by using a scaling analysis approach described elsewhere.[26] This value of R_P is smaller than R_{ON}. For these devices, then, the electrical properties of the source/drain electrodes and their contact resistance with the semiconductor do not strongly influence the transistor performance. The SWNT electrodes have advantages, however, for certain applications as they can exhibit good optical transparency. Also, there is evidence that SWNT–pentacene contacts are more efficient than those formed by Au–pentacene.[27] These differences might become important at channel lengths shorter than those investigated herein.

In conclusion, the combined use of multistream laminar flow in microfluidic channels and controlled flocculation yields a simple but powerful method for depositing and patterning SWNTs in forms ranging from aligned collections of individual tubes to thick network mats. Flow velocities, deposition times, channel geometries, multiphase flows, and dynamic control of flow histories can all be exploited to generate complex patterns of SWNTs that are difficult to construct with other techniques. Working OTFTs that use conducting SWNT lines as source/drain electrodes illustrate one of the possible electronic and sensing devices that can be fabricated.

Experimental Section

SWNT solution: Single-walled carbon nanotubes produced by the laser ablation method were suspended in aqueous sodium dodecyl benzensulfonate (SDBS; 1 wt %).[28] The concentration was typically 10 mg mL^{-1} and no further purification step was carried out after the suspension.

Microfluidic system: A negative photoresist (SU8, Micro Chemical Corp.) of 50-μm thickness was spin-coated onto Si wafers and patterned with high-resolution transparency photomasks by photolithography. PDMS prepolymer and curing agent (Sylgard184, Dow Corning Corp.) (10:1 *w*/*w*) were mixed thoroughly and degassed in vacuum. This solution was poured on the masters (photoresist patterns) and cured at 65 °C for 4 h. After peeling the PDMS molds from the masters, the PDMS molds were either 1) conformably contacted to the substrate by nonspecific surface adhesion forces, or 2) chemically bonded through -OH groups generated by exposing O_2 plasma (O_2 plasma cleaner, Harrick Scientific Corp) on the surface of the PDMS and the SiO_2 surface of the substrate. Chemical bonding was required because the conformal contact was not sufficient to prevent the delamination of the PDMS molds when a curved substrate was used as shown in Figure 3a or when three streams were used as shown in Figure 4b.

Deposition of SWNTs: After 10-nm thick E-SiO_2 was patterned onto T-SiO_2 by the liftoff process, SWNTs were deposited in a microfluidic channel. In this case, the height of the fluidic channel (50 μm) was much higher than the thickness relief (10 nm) of the surface stripe.

Received: May 24, 2005
Revised: September 29, 2005
Published online: December 8, 2005

Keywords: carbon · microfluidics · nanotubes · patterning · transistors

[1] V. Kristic, G. S. Duesberg, J. Muster, M. Burghard, S. Roth, *Chem. Mater.* **1998**, *10*, 2338 – 2340.
[2] Y. Guo, J. Wu, Y. Zhang, *Chem. Phys. Lett.* **2002**, *362*, 314 – 318.
[3] N. P. Armitage, J. C. P. Gabriel, G. Grüner, *J. Appl. Phys.* **2004**, *95*, 3228 – 3230.
[4] Y. Kim, N. Minami, W. Zhu, S. Kazaoui, R. Azumi, M. Matsumoto, *Jpn. J. Appl. Phys.* **2003**, *42*, 7629 – 7634.
[5] M. R. Diehl, S. N. Yaliraki, R. A. Beckman, M. Barahona, J. R. Heath, *Angew. Chem.* **2002**, *114*, 363 – 366; *Angew. Chem. Int. Ed.* **2002**, *41*, 353 – 356.
[6] H. Shimoda, S. J. Oh, H. Z. Geng, R. J. Walker, X. B. Zhang, L. E. McNeil, O. Zhou, *Adv. Mater.* **2002**, *14*, 899 – 901.
[7] M. Burghard, G. Duesberg, G. Philipp, J. Muster, S. Roth, *Adv. Mater.* **1998**, *10*, 584 – 588.
[8] S. G. Rao, L. Huang, W. Setyawan, S. Hong, *Nature* **2003**, *425*, 36 – 37.
[9] M. D. Lay, J. P. Novak, E. S. Snow, *Nano Lett.* **2004**, *4*, 603 – 606.
[10] S. Gerdes, T. Ondarçuhu, S. Cholet, C. Joachim, *Europhys. Lett.* **1999**, *48*, 292 – 298.
[11] S. J. Oh, Y. Cheng, J. Zhang, H. Shimoda, O. Zhou, *Appl. Phys. Lett.* **2003**, *82*, 2521 – 2523.
[12] K. H. Choi, J. P. Bourgoin, S. Auvray, D. Esteve, G. S. Duesberg, S. Roth, M. Burghard, *Surf. Sci.* **2000**, *462*, 195 – 202.
[13] J. Liu, M. J. Casavant, M. Cox, D. A. Walters, P. Boul, W. Lu, A. J. Rimberg, K. A. Smith, D. T. Colbert, R. E. Smalley, *Chem. Phys. Lett.* **1999**, *303*, 125 – 129.
[14] a) H. Ko, S. Peleshanko, V. V. Tsukruk, *J. Phys. Chem. B* **2004**, *108*, 4385 – 4393; b) V. V. Tsukruk, H. Ko, S. Peleshanko, *Phys. Rev. Lett.* **2004**, *92*, 065502.
[15] J. C. Lewenstein, T. P. Burgin, A. Ribayrol, L. A. Nagahara, R. K. Tsui, *Nano Lett.* **2002**, *2*, 443 – 446.
[16] M. A. Meitl, Y. Zhou, A. Gaur, S. Jeon, M. L. Usrey, M. S. Strano, J. A. Rogers, *Nano Lett.* **2004**, *4*, 1643 – 1647.
[17] a) P. J. A. Kenis, R. F. Ismagilov, G. M. Whitesides, *Science* **1999**, *285*, 83 – 85; b) B. Zhao, J. S. Moore, D. J. Beebe, *Science* **2001**, *291*, 1023 – 1026.
[18] R. F. Ismagilov, A. D. Stroock, P. J. A. Kenis, G. M. Whitesides, *Appl. Phys. Lett.* **2000**, *76*, 2376 – 2378.
[19] Z. Fan, S. G. Advani, *Polymer* **2005**, *46*, 5232 – 5240.
[20] Y. Huang, X. Duan, Q. Wei, C. M. Lieber, *Science* **2001**, *291*, 630 – 633.
[21] N. Saran, K. Parikh, D. Suh, E. Muñoz, H. Kolla, S. K. Manohar, *J. Am. Chem. Soc.* **2004**, *126*, 4462 – 4463.
[22] E. S. Snow, J. P. Novak, P. M. Campbell, D. Park, *Appl. Phys. Lett.* **2003**, *82*, 2145 – 2147.
[23] Y. Zhou, A. Gaur, S. H. Hur, C. Kocabas, M. A. Meitl, M. Shim, J. A. Rogers, *Nano Lett.* **2004**, *4*, 2031 – 2035.
[24] C. Kocabas, M. A. Meitl, A. Gaur, M. Shim, J. A. Rogers, *Nano Lett.* **2004**, *4*, 2421 – 2426.
[25] L. Hu, D. S. Hecht, G. Grüner, *Nano Lett.* **2004**, *4*, 2513 – 2517.
[26] J. Zaumseil, K. W. Baldwin, J. A. Rogers, *J. Appl. Phys.* **2003**, *93*, 6117 – 6124.
[27] M. Lefenfeld, G. Blanchet, J. A. Rogers, *Adv. Mater.* **2003**, *15*, 1188 – 1191.
[28] V. C. Moore, M. S. Strano, E. H. Haroz, R. H. Hauge, R. E. Smalley, *Nano Lett.* **2003**, *3*, 1379 – 1382.

